Single-molecule analysis of cadherin-mediated cell-cell adhesion

Porntula Panorchan[1], Melissa S. Thompson[1], Kelly J. Davis[1], Yiider Tseng[2], Konstantinos Konstantopoulos[1,*] and Denis Wirtz[1,*]

[1]Department of Chemical and Biomolecular Engineering, The Johns Hopkins University, 3400 N. Charles Street, Baltimore, MD 21218, USA
[2]Department of Chemical Engineering, University of Florida, Gainesville, FL 32611, USA
*Authors for correspondence (e-mail: kkonsta1@jhu.edu; wirtz@jhu.edu)

Accepted 28 September 2005
Journal of Cell Science 119, 66-74 Published by The Company of Biologists 2006
doi:10.1242/jcs.02719

Summary

Cadherins are ubiquitous cell surface molecules that are expressed in virtually all solid tissues and localize at sites of cell-cell contact. Cadherins form a large and diverse family of adhesion molecules, which play a crucial role in a multitude of cellular processes, including cell-cell adhesion, motility, and cell sorting in maturing organs and tissues, presumably because of their different binding capacity and specificity. Here, we develop a method that probes the biochemical and biophysical properties of the binding interactions between cadherins expressed on the surface of living cells, at the single-molecule level. Single-molecule force spectroscopy reveals that classical cadherins, N-cadherin and E-cadherin, form bonds that display adhesion specificity, and a pronounced difference in adhesion force and reactive compliance, but not in bond lifetime. Moreover, their potentials of interaction, derived from force-spectroscopy measurements, are qualitatively different when comparing the single-barrier energy potential for the dissociation of an N-cadherin–N-cadherin bond with the double-barrier energy potential for an E-cadherin–E-cadherin bond. Together these results suggest that N-cadherin and E-cadherin molecules form homophilic bonds between juxtaposed cells that have significantly different kinetic and micromechanical properties.

Key words: Cell adhesion, Cadherins, Biophysics, Single-molecule force spectroscopy

Introduction

Cadherins are expressed in virtually all solid tissues and play a key role in a wide range of physiological and pathological processes. These calcium-dependent cell-surface molecules cluster at sites of cell-cell contact where they mediate cell adhesion and signaling, and subsequently influence other cell processes such as motility, differentiation and carcinogenesis (Adams and Nelson, 1998). Given the different expression patterns in vivo and based on aggregation assays in which cells expressing different cadherins separate and form distinct colonies in vitro, it has long been speculated that cadherins interact only through homophilic interactions and that different cadherins have different binding capacities (Gumbiner, 1996; Nose et al., 1990; Tamura et al., 1998). Differential binding capacity and adhesion specificity of cadherins are thought to be responsible for the formation of tissue boundaries and cell sorting in developing tissues (Duguay et al., 2003; Gumbiner, 1996). However, recent results suggest that cadherins are more promiscuous than previously suspected. Cadherins seem to be able to bind through heterophilic interactions (Shan et al., 2000; Shimoyama et al., 1999). Moreover, experiments using adhesion assays combined with an aggregation assay suggest that the extent of cell sorting neither correlates with binding capacity nor adhesion specificity (Niessen and Gumbiner, 2002). Nevertheless, the fundamental question of whether individual cadherin molecules display differential binding and adhesion specificity at the single-molecule level rather than the cell level, remains unanswered.

N-cadherin and E-cadherin are the prototypical members of classical type I cadherins, which mediate cell-cell adhesion at adherens junctions and are linked to the actin cytoskeleton through $p120^{ctn}$, β-catenin and α-catenin (Nelson and Nusse, 2004). When co-cultured, cells expressing N-cadherin and E-cadherin separate into distinct aggregates. N-cadherin is not typically expressed by normal epithelial cells, which express primarily E-cadherin. However, N-cadherin is detected in breast cancer cells of epithelial origin and increases tumor cell migration and invasion in vitro (Wheelock et al., 2001). To test whether N- and E-cadherin can bind through both homophilic and heterophilic interactions and test whether cadherin molecules display differential binding capacity, both at the single-molecule level, we use a method that directly measures the lifetime and adhesion force of individual bonds made of single homotypic cadherin pairs expressed on the surface of apposing cells. The single-molecule analysis presented here resolves pair-wise molecular interactions from global cell-cell interactions and examines the contribution of individual molecules (acknowledging molecular 'individuality') instead of describing average behavior. Moreover, the use of living cells rather than recombinant proteins (Baumgartner et al., 2000; Baumgartner et al., 2003; Perret et al., 2004) ensures proper molecular orientation and preserves post-translational modifications of cell-surface molecules. Our single-molecule force spectroscopy measurements reveal that N-cadherin and E-cadherin show adhesion specificity, i.e. an N-cadherin pair cannot form a functional bond with an E-cadherin pair.

N-cadherin–N-cadherin and E-cadherin–E-cadherin bonds display pronounced differences in adhesion force and reactive compliance, but not in bond lifetime. Together these results suggest that classical type I N- and E-cadherins form bonds that exhibit significantly different kinetic and micromechanical properties.

Results

Analysis of cadherin-cadherin interactions in live cells at the single-molecule level

Pair-wise cadherin-cadherin binding interactions on apposing cells are characterized at the single-molecule level using a molecular force probe (MFP) (Fig. 1A) (Hanley et al., 2003). Using a microinjector equipped with a microneedle, we deposited individual biotinylated cadherin-expressing cells onto a cantilever pre-coated with streptavidin (Fig. 1B,C). The cantilever was then positioned over a target cell and was approached to establish contact. The time of contact between the cells was short to allow for the establishment of either none or very few bonds. Upon retraction of the cantilever, the breakage of cadherin bonds between cells caused deflections of the cantilever, which were translated into time-dependent forces and recorded as a function of the distance between cells. Typical force-displacement spectra are shown in Fig. 2. For each type of cadherin assayed and for each tested reproach velocity, hundreds of force-displacement spectra (n>500) were collected and analyzed to extract rupture forces (i.e. the height of the discrete force step at rupture, inset Fig. 3A) and loading rates, which were subsequently pooled into histograms (e.g. Fig. 4A).

To ensure that the biotinylation of cell-surface molecules did not alter the functionality of N-cadherins, we tested the

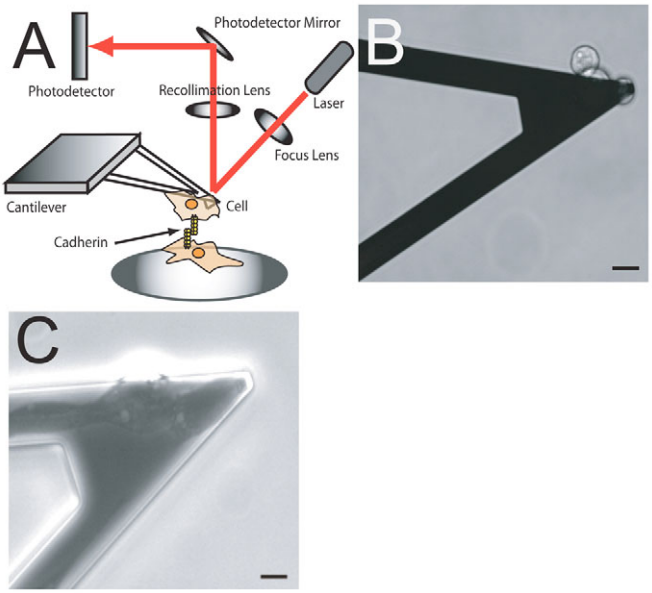

Fig. 1. Principle of single-molecule force spectroscopy measurements in living cells. (A) Schematic of the molecular force probe (MFP) used here to probe cadherin-mediated cell-cell interactions at the single-molecule level. (B) Phase-contrast microscopy of cadherin-expressing CHO cells deposited on a cantilever. (C) Phase-contrast microscopy of adherent CHO cells attached to the end of a cantilever. Scale bars, 15 μm (B); 10 μm (C).

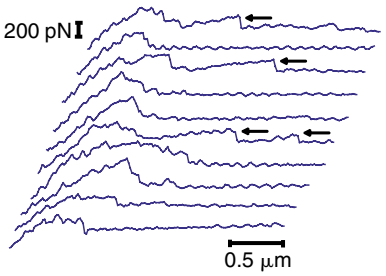

Fig. 2. Force-distance spectra for cadherin/cadherin bonds. Typical force-distance curves during the forced de-adhesion of two apposing E-cadherin cells at a constant cantilever reproach velocity of 25 μm/second. One cell is attached to the cantilever of the MFP (shown in Fig. 1); the other cell is plated on a culture dish. Arrows indicate the rupture of cadherin bonds. Only curves showing a single clear bond rupture were analyzed.

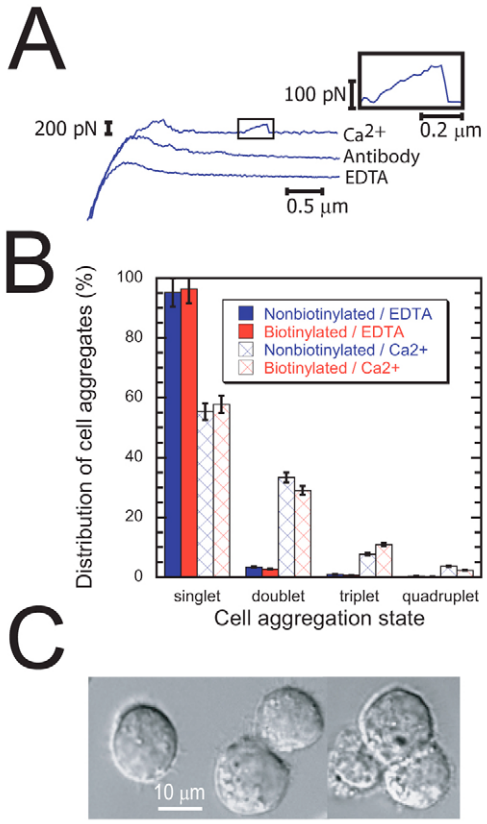

Fig. 3. Interaction between apposing cells are specific and involve cadherins. (A) Force-distance curves for cells with and without either EDTA or anti-E-cadherin function-blocking monoclonal antibodies (ECCD-1). Inset shows the force peak, from which rupture force (height of the peak) and loading rate (reproach velocity of the cantilever times the rate of increase before rupture) are obtained. (B) Distribution of N-cadherin cell aggregates, as assessed by flow cytometry. This graph shows that the biotinylation process does not change the distribution of cell aggregates and, therefore, the functionality of cadherins is unaffected by biotinylation. Solid bars represent conditions where EDTA is added to the solution; hatched bars represent conditions where calcium is added. Blue bars represent non-biotinylated cells; red bars represent biotinylated cells. (C) Phase-contrast micrograph of cells in different aggregation states. Bar, 10 μm.

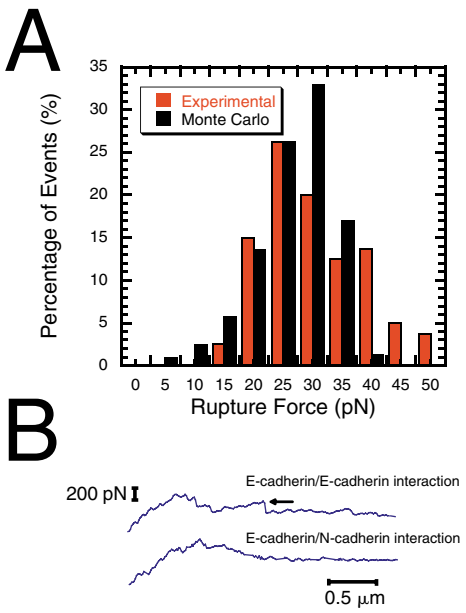

Fig. 4. Experimental and theoretical rupture force distribution of a cadherin-cadherin bond and heterotypic cadherin-cadherin interactions. (A) Experimental (white) and theoretical (black) histograms of rupture forces to break a single N-cadherin–N-cadherin bond connecting two apposing cells at a cantilever reproach velocity of 5 μm/second. Monte Carlo simulations, which were conducted using the Bell's model unstressed off-rate and reactive compliance extracted from the plot shown in Fig. 6A, show the consistency of the experimental data with the Bell's model predictions and further indicate that only one single type of bond is analyzed. (B) Representative force-distance curves for the detachment between two E-cadherin cells (top curve) and between an E-cadherin cell and an N-cadherin cell (bottom curve).

biotinylated cells with a cell aggregation assay based on flow cytometry (Fig. 3B). In the presence of EDTA, N-cadherin-expressing cells did not aggregate and exhibited a large population of single (i.e. non-aggregated) cells (95.8±4.9%). In the presence of calcium, cells aggregated extensively and organized into singlets (56.5±2.8%), doublets (31.2±1.6%), triplets (9.3±0.5%) and quadruplets (2.9±0.2%) (mean ± s.e.m.; n=4). Importantly, we found no significant differences in the extents of aggregation between biotinylated cells and non-biotinylated cells (Fig. 3B). Cells were also examined by phase-contrast microscopy for qualitative confirmation of these results (Fig. 3C). Moreover, both non-biotinylated and biotinylated cells were treated with an anti-N-cadherin-specific antibody, which were then tagged with a fluorescent secondary antibody for flow cytometry analysis. The intensity measured by flow cytometry values were 521±9 and 531±2 (mean ± s.e.m.; n=3) for control and biotinylated cells, respectively. This difference is insignificant (P>0.05) and indicates that the biotinylation process did not affect the binding of a specific antibody or the level of cadherin expression on the surface of the cells. For E-cadherin cells, the cells were biotinylated prior to induction with dexamethasone. Thus, E-cadherin molecules expressed on the cell surface were not biotinylated. E-cadherin and N-cadherin cells were left overnight to incubate in culture medium in 5% CO_2 at 37°C, which restored cadherin expression on the cell surface prior to the experiment.

We verified the specificity of cadherin-mediated cell interactions probed by the MFP by treating the cells with either anti-E-cadherin (ECCD-1) or anti-N-cadherin (NCD-2) functional-blocking monoclonal antibodies, respectively. For both N- and E-cadherin cells, the treatment with monoclonal antibodies significantly reduced the frequency of binding interactions, from approximately 30% to less than 5%, with rupture forces below the detection level of the MFP (<4 pN; n=300 each). Force-displacement curves were similar to those obtained with control cells with EDTA, displaying low background, non-specific binding (Fig. 3A). Therefore, in the conditions of this study, adhesive interactions between apposing cells only involved specific cadherin-mediated binding interactions.

The extent of adhesion between apposing cells depended on both their interaction time and the impingement force applied by the computer-controlled cantilever on the target cell. To control the impingement force, we adjusted the starting and final positions of the cantilever. With lower impingement forces, the contact area between cells decreased, which diminished the number of bonds between cells (i.e. qualitatively detected by the number of bond rupture events on force-displacement spectra). Short interaction times also decreased the number of bonds that are formed between apposing cells (Chu et al., 2004). A recent study using recombinant proteins (Perret et al., 2004) suggests that the adhesion force between individual E-cadherin molecules depends on their time of interaction. Here we promote single-bond engagement between apposing cells as opposed to multiple bonds by letting cells interact only for an extremely short time (1 msecond) to target a percentage of successful cell-cell interactions (i.e. those producing a rupture event) of 10-30%. Based on Poisson distribution statistics, when 30% of cell-cell contact leads to cadherin/cadherin binding, >80% of successful binding events involve a single bond, 15% involve double bonds and <3% involve triple bonds (Chesla et al., 1998). This analysis applies to any ligand-receptor pair, including cadherins studied here and selectins studied earlier (Hanley et al., 2003; Hanley et al., 2004). To further reduce the contact area between cells, the maximal impingement force applied by the cantilever during approach was reduced to 200 pN (Benoit et al., 2000; Sako et al., 1998). Inspection of force-displacement spectra readily distinguish single bond interactions from rare multiple-bond interactions between apposing cells: the former involves a single rupture event (marked by an abrupt force drop marked by an arrow in Fig. 2), the latter involves multiple bond ruptures (arrows in Fig. 2). We also verified that the rupture force histogram obtained at each reproach velocity (Fig. 5A,B) displayed a unique well-defined peak as opposed to multiple quantized peaks (Benoit et al., 2000) (see also Monte Carlo simulations below). Together these precautions ensured that cell-cell adhesion in our assay involved one type of molecular bond, that non-specific interactions between cells were insignificant, and that only parameters characterizing individual cadherin-cadherin bonds between apposing cells were analyzed.

Formation of a single cadherin-cadherin bond requires calcium

Calcium promotes homodimerization of cadherin molecules in vitro (Patel et al., 2003) and is required to mediate overall cell-

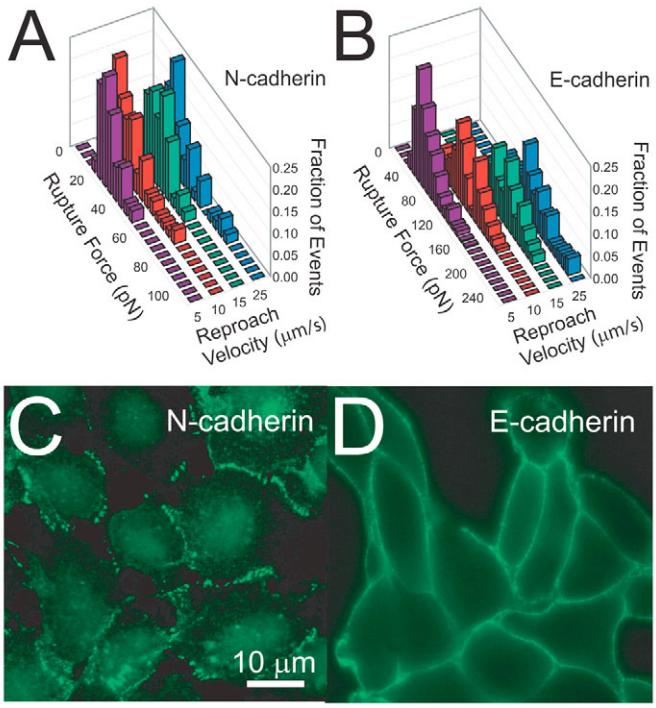

Fig. 5. Rupture force of a single cadherin-cadherin bond as a function of reproach velocity. (A) Distribution of rupture forces to break a single E-cadherin–E-cadherin bond between apposing cells subjected to different reproach velocities, representing at least 500 cell-cell contacts at each velocity. (B) Distribution of rupture forces to break a single N-cadherin–N-cadherin bond at different reproach velocities, representing at least 500 cell-cell contacts at each velocity. Immunofluorescence micrographs of N-cadherin-expressing CHO cells (C) and E-cadherin-expressing CHO cells (D). Bar, 10 μm.

cell adhesion and promote multiple adhesive bonds (Gumbiner, 1996; Sivasankar et al., 1999; Takeichi, 1991). These earlier studies tested global cell-cell adhesion, which may depend not only on molecular cadherin/cadherin interactions, but also on calcium-mediated changes in cadherin re-organization and clustering on the cell surface. To test the requirement of calcium for molecular interactions between cadherin pairs on apposing cells, the chelating agent EDTA was added to the tissue culture. The addition of EDTA was found to completely abrogate cadherin-cadherin binding; no successful adhesion event occurred and no significant rupture force (>3 pN) was recorded (n=300) (Fig. 3A). These results show that binding interactions between individual cadherins on apposing cells require calcium.

Bond lifetime and adhesion force: N-cadherin–N-cadherin vs E-cadherin–E-cadherin bonds

To characterize and compare homophilic interactions between cadherins, critical biochemical and biophysical parameters for each of the molecular pairs E-cadherin–E-cadherin and N-cadherin–N-cadherin were evaluated using Bell's model. This model relates the bond rupture force to the loading rate applied to cell-surface molecules (Bell, 1978; Evans and Ritchie, 1997). The same model has been successfully used, for instance, to characterize binding interactions between adhesion molecules on the surface of cells and purified ligands involved in inflammation and blood-borne metastasis (Alon et al., 1995; Evans, 2001; Hanley et al., 2003) (Table 1). The mean rupture force, f_m, is plotted as a function of the natural log of the loading rate, r_f (Fig. 6A) (Bell, 1978; Evans and Ritchie, 1997):

$$f_m = \frac{k_B T}{x_\beta} \ln\left(\frac{x_\beta}{k^0_{off} k_B T}\right) + \frac{k_B T}{x_\beta} \ln(r_f)\,, \qquad (1)$$

where k_B is the Boltzmann constant and T is the absolute temperature. The unstressed dissociation rate, k^0_{off} and the potential length of the transition state (also called reactive compliance), x_β, were extracted by fitting rupture-force measurements as a function of loading rate to Eq. 1. We note that, although MFP measurements were collected under non-zero loading rate, data extrapolation to zero loading rate yields an unstressed (equilibrium) dissociation rate.

To further test the consistency of our data with Bell's model predictions, Monte Carlo simulations of receptor-ligand bond rupture under constant loading rates were performed, following a procedure described (Hanley et al., 2004). Ten thousand rupture forces (F_{rup}=r_f $n\Delta t$) were calculated, for which the probability of bond rupture P_{rup}:

$$P_{rup} = 1 - \exp\left[-k^0_{off} \exp\left(\frac{x_\beta r_f n\Delta t}{k_B T}\right)\Delta t\right], \qquad (2)$$

was greater than P_{ran}, a random number between zero and one. Here Δt is the interval and $n\Delta t$ is the time step and k^0_{off} and x_β are those obtained experimentally. Simulated and experimentally obtained rupture force distributions and mean rupture forces agreed, as shown for a representative experimental condition and Monte Carlo simulations for N-cadherin–N-cadherin binding at a reproach velocity of 5 μm/second (Fig. 4A). The distributions of rupture forces obtained from experiments and Monte Carlo simulations both show one peak and a relatively large width. Since the simulated distribution was obtained using as a single dissociation rate and reactive compliance, the excellent agreement between computational and experimental distributions indicates that their relatively large widths stem from natural dispersion, not from the adhesion of multiple bonds.

Our single-molecule analysis suggests that, in living cells, N-cadherin and E-cadherin molecules show a qualitative and quantitative difference in their binding mechanism. One can recast qualitatively the force-loading rate curves into interaction potentials (Fig. 6B) (Hummer and Szabo, 2001). N-cadherin molecules on apposing cells interact through a single-barrier interaction potential (Fig. 6B). Indeed, within the range of tested loading rates, the force required to break an N-cadherin–N-cadherin bond grew linearly with the natural log of the loading rate (Fig. 6A), which corresponds to an intermolecular potential with a single activation energy barrier. In striking contrast to N-cadherin, our single-molecule analysis suggests that E-cadherin molecules on apposing cells interact through a double-barrier interaction potential (see schematic, Fig. 6B). The rupture force of the E-cadherin–E-cadherin bond also grew linearly with the natural log of the loading rate, but at two different slopes before and after a threshold loading rate of ~500 pN/second (Fig. 6A).

The E-cadherin–E-cadherin bond could withstand mean forces up to 73 pN for a loading rate of 1000 pN/second and

Table 1. Single-molecule cadherin-cadherin pair-wise interactions in living cells

Molecular pair	Mean bond rupture forces (pN)	Rate of bond dissociation, k^0_{off} (seconds^{-1})	Bond lifetime (seconds)	Reactive compliance, x_β (nm)	Reference
N-cadherin–N-cadherin	30 40	0.98±0.46	1.02±0.48	0.77±0.09	This work
E-cadherin–E-cadherin	73 157	1.09±0.35 4.00±0.68	0.92±0.29 0.25±0.04	0.32±0.07 0.10±0.02	This work
P-selectin–PSGL-1	147 230	0.22±0.05	4.55±1.24	0.14±0.01	Hanley et al., 2004
P-selectin–LS174T ligand	80 160	2.78±0.02	0.36±0.002	0.13±0.01	Hanley et al., 2003

The first and second values of mean bond rupture forces are evaluated at the loading rates of 1000 pN/second and 10,000 pN/second, respectively. The slope of Eq. 1 yields the separation distance along the reaction coordinate, x_β, which is related to the reactive compliance of the bond, and the unstressed dissociation rate k^0_{off}, which is obtained from the extrapolation of the curve to zero force. The two values of k^0_{off} and x_β for E-cadherin–E-cadherin bond correspond to low (<500 pN/second) and high loading rates (>500 pN/second) (Fig. 6A). The errors for k^0_{off} and x_β were computed using the method of random-variable realizations. For comparison, we report the tensile strength, dissociation rate, lifetime, and reactive compliance of the P-selectin–PSGL-1 bond and P-selectin–LS174T ligand bond, which are involved in inflammation and blood-borne metastasis, respectively.

157 pN for a loading rate of 10,000 pN/second (Fig. 6A). By contrast, the N-cadherin–N-cadherin bond could only withstand forces up to 30 pN and 40 pN for the same loading rates. Fitting the data using Eq. 1 yielded an unstressed (single) dissociation rate of 0.9 second^{-1} and a reactive compliance (also called transition potential length) of 7.7 angstroms for the N-cadherin molecular pair. For the E-cadherin molecular pair, the unstressed dissociation rate constant was 1.1 second^{-1} at low loading rates (<500 pN/second) and 4.0 second^{-1} at high loading rates (>500 pN/second) (Table 1). The transition potential length of interaction for an E-cadherin pair was 3.2 angstroms at low loading rates and 1.0 angstrom at high loading rates. We note that measurements with CHO cells expressing E-cadherin led to the same mean rupture forces, reactive compliance and dissociation rates (P>0.05) as those obtained with L-M(TK-) E-cadherin cells. The comparison between E- and N-cadherin homophilic interaction parameters are summarized as follows (see also Table 1): tensile strength, EE>NN (rupture force, f_m); bond lifetime, EE~NN (1/dissociation rate constant, $1/k^0_{off}$); probability of rupture, EE<NN (reactive compliance, x_β).

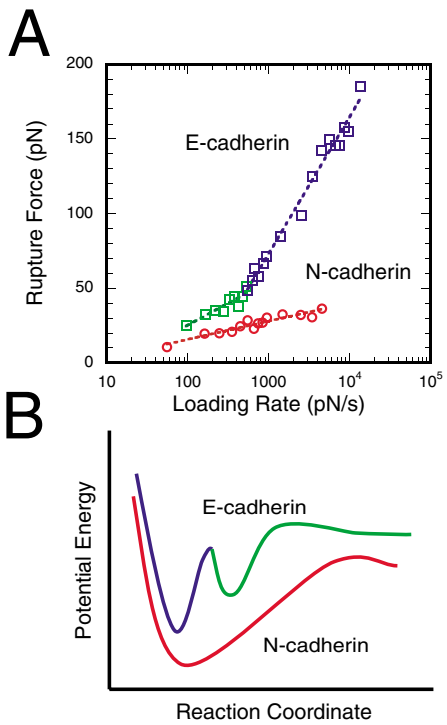

Fig. 6. Single-bond analysis of cadherin-mediated cell-cell adhesion. (A) Mean rupture force of a single bond as a function of loading rate. Curve fitting with Bell's model allows for the computation of the unstressed dissociation rate, k^0_{off} and the reactive compliance, x_β, of a bond. (B) Schematic of the intermolecular potential of interaction between E-cadherin pairs and N-cadherin pairs on apposing cells. This energy potential is qualitatively based on data shown in A. Blue represents the inner barrier potential at high loading rates; green represents the outer barrier potential at low loading rates for the dissociation of a single E-cadherin/E-cadherin bond between cells; red represents the single barrier potential to be overcome for the dissociation of a single N-cadherin–N-cadherin bond. The width of each potential well is taken as the reactive compliance.

A similar unstressed dissociation rate implies that an individual E-cadherin–E-cadherin bond connecting two cells has a similar lifetime as the N-cadherin–N-cadherin bond. A lower reactive compliance and higher rupture force imply that E-cadherin–E-cadherin bonds between apposing cells are less prone to rupture than N-cadherin–N-cadherin bonds.

To test whether morphological changes of the cells, such as microvillus extensions during pulling, could have on our analysis, cells were fixed with 1% formalin (Hanley et al., 2003). The process of fixing cells diminishes the likelihood that the applied load on the cadherin-cadherin complex is partially dissipated by viscous deformation during microvillus extension. Thus, the rupture forces for fixed cells may be higher at all loading rates than for unfixed cells, because nearly the entire applied load is placed on the cadherin pairs and cytoskeletal contribution is eliminated. However, our experiments reveal that neither the tensile strength at all loading rates nor the Bell's model parameters were changed by cell fixation (data not shown).

Heterophylic interactions between E-cadherin and N-cadherin do not occur

Previous studies using cell aggregation assays suggest that heterophilic interactions between N-cadherin and E-cadherin

reduce global cell-cell adhesion (Duguay et al., 2003; Shan et al., 2000). To investigate whether heterophilic binding interaction between a single N-cadherin dimer and a single E-cadherin dimer between apposing cells could occur, an E-cadherin cell was placed on the cantilever and N-cadherin cells were plated on the bottom tissue culture plate. The alternative arrangement where an N-cadherin cell was placed on the cantilever did not change the outcome. The frequency of binding of heterophilic N-cadherin–E-cadherin interactions was very low compared to homophilic interactions, <5% for reproach velocities 5 μm/second<v<25 μm/second (n=300 cell-cell contacts for each velocity). This is within the range of non-specific binding obtained in the presence of function-blocking antibodies against cadherins and with control cells not expressing cadherins. Representative force-distance curves for the binding between E-cadherin cells and between E-cadherin and N-cadherin cells are shown in Fig. 4B. These results suggest that heterophilic interactions between single E- and N-cadherin pairs on apposing cells did not occur.

Discussion

In this study, we compared the homophilic and heterophilic binding capabilities of classical type I cadherins, E-cadherin and N-cadherin. Using a single-molecule analysis, we showed that individual classical E- and N-cadherin pairs display different biochemical and biophysical properties. The E-cadherin–E-cadherin bond has a significantly lower reactive compliance and a much higher tensile strength than the N-cadherin–N-cadherin bond, which translates into higher resistance of E-cadherins to bond rupture in the presence of mechanical stress. Moreover, the forced disengagement of E-cadherin dimers from each other proceeds through a two-step process. In contrast, the N-cadherin–N-cadherin bond under tension breaks in a continuous manner (at least within the probed range of loading rates). In the absence of force, the E-cadherin–E-cadherin bond has a similar dissociation rate with that of the N-cadherin–N-cadherin bond, which indicates a similar bond lifetime. The effect of force on the cadherin-cadherin bond lifetime could be probed directly by adapting for living cells the approach recently introduced by Zhu and co-workers (Konstantopoulos et al., 2003; Marshall et al., 2003; Yago et al., 2004).

The extracellular homophilic-binding domain of cadherins consists of five tandem repeats (EC1-EC5). Some controversy remains regarding how and which EC domains contribute to the global binding interactions between cadherin molecules. The conventionally accepted linear zipper model attributes the adhesion of cadherins to the most distal EC1 and EC2 domains (Makagiansar et al., 2002; Pertz et al., 1999; Shapiro et al., 1995). However, recent studies have suggested the crucial involvement of other EC domains for a stable cadherin adhesion (Chappuis-Flament et al., 2001; Perret et al., 2004; Shiraishi et al., 2005; Sivasankar et al., 1999). Using a surface force apparatus, cadherins immobilized on atomically smooth surfaces have been shown to unbind through three discrete jumps of length comparable to EC domain dimensions upon separation (Sivasankar et al., 1999; Sivasankar et al., 2001). Moreover, based on results obtained with purified C-cadherin fragments and bead-aggregation and cell-adhesion assays, a model was proposed in which multiple EC domains are required for stable cadherin interactions (Chappuis-Flament et al., 2001). More closely related to our single-molecule measurements are the previous tests of interactions between full-length (EC1-5) and fragment (EC1-2) E-cadherin (Perret et al., 2004) and full-length vascular endothelial-cadherins (VE-cadherin) by AFM (Baumgartner et al., 2000). At low loading rates (100-500 pN/second), our data for N-cadherin and E-cadherin yielded forces similar to those reported by Baumgartner et al. for VE-cadherin and Perret et al. for the weak, ‘sub-state’ of EC1-2/EC1-2 interactions. Our results show that at higher loading rates (>1000 pN/second), N-cadherin kinetics remains similar to that at low loading rates, whereas E-cadherins exhibit different binding kinetics. In agreement with Perret et al. for EC12, we found two sub-states of E-cadherin binding at slow and very fast loading rates. For fast loading rates, broader distributions of rupture forces were observed. We did not observe higher strength or additional sub-states of cadherin adhesion, which may be due to our use of short interaction times. The short contact time used here was necessary to avoid the formation of multiple bonds and allows for the observation of cadherin interactions at the single-molecule level. Another possible explanation may be that unlike previous studies, we probe live cells, for which cadherins possess transmembrane and cytoplasmic domains that can interact with cytoplasmic structures. Indeed, several studies have shown that the adhesive strength of cadherin is regulated by these domains (Huber et al., 1999; Ozawa, 2002; Yap, 1998; Yap et al., 1997). The present results provide direct support for the notion that different cadherins display different binding kinetics and biophysical properties. How different EC domains contribute to the adhesion of individual cadherin molecules could be tested in the future with cadherin mutants (EC domain deletion) expressed on live cells.

Our results seemingly contradict conclusions drawn from results obtained using an adhesion assay that flows cadherin-expressing cells above plates coated with immobilized cadherin molecules (Niessen and Gumbiner, 2002), which revealed no significant difference in the binding capacity of cadherins. It was concluded that cell sorting was primarily determined by mechanisms different from binding or adhesion specificity (Niessen and Gumbiner, 2002). Our conclusion is only superficially different from that of these authors. Different cadherins were assayed and the flow assay estimates global cell-cell adhesion (avidity) while the assay used here measures single-molecular interactions.

The binding specificity and difference in the micromechanics of E-cadherin–E-cadherin and N-cadherin–N-cadherin bonds formed between juxtaposed cells suggest a physical basis for the change in cadherin expression observed in epithelial cells undergoing malignant transformation (Cavellero and Christofori, 2004). N-cadherin is not typically expressed by epithelial cells. However, N-cadherin is detected in breast cancer cells of epithelial origin and it increases tumor cell migration and invasion in vitro (Wheelock et al., 2001). Our results suggest that metastatic cells may express N-cadherins because these adhesion molecules form homophilic bonds that are less resistant to bond rupture under physiological stress conditions, thus assisting transformed cells to break away from their neighbors in the primary tumor. By analogy with a car wheel spinning in mud that needs some reasonable traction to move forward, the lower bond rupture force, but larger transition potential length, of the N-

cadherin–N-cadherin bond provides highly invasive cells with a sliding and peeling bond-breakage mechanism, which may aid them in generating productive forward motion to escape their local tumor environment. The existence of two different sub-states of E-cadherin bond kinetics may reflect the different functions of E-cadherin. A high dissociation rate, fast release sub-state of E-cadherin may be useful for rapid, cell-recognition processes, which occur during cell sorting in developing tissues. The more stable, longer bond lifetime sub-state may be used to establish stable long-lived junctions once a suitable binding partner is found.

To place our single-molecule measurements of binding interactions between cadherins in context, we compare the kinetic and micromechanical properties of cadherin-cadherin bonds with those of molecular bonds, P-selectin–PSGL-1 and P-selectin–LS174T cell ligand (Table 1). These bonds play a key role in cell-cell adhesion in leukocyte-endothelium interactions during inflammation and carcinoma-endothelium interaction during metastasis, respectively. The kinetic and micromechanical properties of these bonds were assayed at the single-molecule level with intact cells, using the same instrument (Hanley et al., 2003; Hanley et al., 2004). Forces acting on cadherin bonds, which are involved in (epithelial and endothelial) cell-cell adhesion, are expected to be relatively low. By contrast, upon binding to the activated endothelium, leukocytes and cancer cells have to resist hemodynamic flows, which subject P-selectin-ligand bonds to high forces. Our single-molecule measurements of bond tensile strength are consistent with the distinct functions played by cadherins and selectins in cell-cell adhesion.

Cadherin-mediated cell-cell adhesion may be further modulated by the regulated binding of cytoplasmic molecules, such as proteins $p120^{ctn}$ and β-catenin, to the cytoplasmic domain of cadherins (Ireton et al., 2002; Nelson and Nusse, 2004; Shapiro, 2001). The effect of cadherin signaling on cadherin-mediated cell-cell adhesion could be investigated at the single molecule level with the method used here to investigate the putative regulatory role of cadherin-binding proteins, which may promote inside-out signaling.

Materials and Methods

Cell culture

Chinese hamster ovary (CHO) cells expressing full-length N-cadherin were kindly provided by G. Borisy (Northwestern University, IL) (Chausovsky et al., 2000) and grown in Dulbecco's modified Eagle's medium (DMEM; ATCC, Manassas, VA) supplemented with 10% bovine calf serum (BCS, ATCC) and 1 mg/ml G418 (Mediatech, Herndon, VA) in 5% CO_2 at 37°C. Mouse L-M(TK-) cells expressing full-length E-cadherin were kindly provided by W. J. Nelson (Stanford University, CA) and grown in the same medium except with 0.3 mg/ml G418. We also conducted experiments with CHO cells expressing full-length E-cadherin and obtained the same kinetic and mechanical properties within SEM as for L-M(TK-) cells (data not shown). Prior to experimenting, L-M(TK-) cells were induced overnight with dexamethasone (Sigma-Aldrich, St Louis, MO) to a final concentration of 1 μM for maximal expression of E-cadherin (Angres et al., 1996). Cells were removed from culture flasks with cell dissociation buffer (Invitrogen) for 10 minutes at 37°C. For MFP experiments, 200 μl of 1×10^6 cells/ml cell suspension was added to 60 mm tissue culture dishes containing 5 ml culture media and incubated overnight in 5% CO_2 at 37°C to allow cell spreading and restoration of cadherins. Immediately before the molecular force probe experiment, the media was changed to serum-free media containing 4-(2-hydroxyethyl)-1-piperazineethanesulfonic acid (HEPES) (Invitrogen) to stabilize the pH while outside of the 5% CO_2 environment of the incubator.

Biotinylation of cell surface molecules

Streptavidin-biotin linkages were used to tether cells on the cantilever. Biotinylation of cell surface molecules was performed as described previously (Altin and Pagler, 1995). Briefly, cells were washed three times with ice-cold PBS, then incubated in 0.5 mg/ml sulfo-NHS-LC-biotin (Pierce, Rockford, IL) for 30 minutes at room temperature. Any remaining biotinylation reagent was removed by centrifugation and subsequently washing the cells three times with ice-cold PBS. Con-A-mediated cell attachment led to identical kinetic and mechanical Bell's model parameters.

Cantilever preparation

A Silicon nitride AFM cantilever (Veeco Instruments, Woodbury, NY) was washed with 10% HCl/70% ethanol solution, distilled water, and 95% ethanol solution each for 1 minute. The cantilevers were subsequently washed with acetone and distilled water for 5 minutes each and then incubated in 0.5 mg/ml streptavidin (Pierce) overnight at 20°C.

Cell attachment to the cantilever

Using an Eppendorf Transjector 5246 (Brinkmann Instruments, Westbury, NY) equipped with the streptavidin-coated (0.2 mg/ml streptavidin), modified borosilicate microneedle (World Precision Instruments, Sarasota, FL) (Rahman et al., 2002), a biotinylated cell was detached from of its culture dish and placed onto the sharp end of the cantilever (Fig. 1A,B). The cell attachment process was performed under a 10× Plan Fluor objective (NA 0.3). The cantilever was then incubated in culture medium in 5% CO_2 at 37°C overnight to allow cell spreading on the cantilever (Fig. 1C).

Single-molecule force spectroscopy

Single-molecule experiments were conducted using a molecular force probe (MFP; Asylum Research, Santa Barbara, CA; Fig. 1A) (Chang et al., 2005; Hanley et al., 2003). The MFP is a piconewton-sensitive instrument that measures adhesion forces as a function of cantilever tip to sample separation distance. MFP utilizes a flexible cantilever tip, which deflects in response to forces between the tip and sample surface. Deflections were detected by a laser focused onto the cantilever and translated into time-dependent forces using the cantilever bending constant. The time-dependent deflection of the cantilever was determined by laser deflection onto a photodetector occurred at a rate of 1.0 kHz. Each cantilever was calibrated by the nondestructive thermal oscillation method before use (Hutter and Beccoeffer, 1993); the cantilever had a mean bending constant of 10 pN/nm.

Two outputs are generated from MFP experiments: the photodetector (PSPD) sensor output (V) and the linear variable differential transformer (LVDT) output. The PSPD sensor output is translated into cantilever deflection (nm) by multiplying the sensor output with the inverse optical lever sensitivity (Inv OLS), which is the inverse slope of the sensor output versus the LVDT output curve in the constant compliance regime. The LVDT output is translated into the tip-sample separation distance by taking the difference between the total cantilever movement and the displacement due to the applied force. The force measured from the cantilever deflection is calculated based on Hooke's Law for linear elastic springs, $F=k\Delta x$, where F is the force (expressed in piconewtons, pN), k is the known bending constant of the cantilever (~10 pN/μm), and Δx is the measured deflection (nm).

Single-molecule data acquisition and analysis

With a culture dish placed on the MFP bottom stage, the cantilever bearing a few cells was positioned over a target cell and was approached to establish contact of a preset duration. Upon retraction, cell-cell interactions caused deflections of the cantilever, which were translated into forces and recorded as a function of displacement from the point of contact to the total separation of the cells. The pulling velocity was varied from 1 to 30 μm/second. The dwell time was set to 1 msecond to minimize the occurrence of multiple events. By adjusting the final position of the cantilever, we limited the force of approach (i.e. impingement force) to 200 pN. Rupture forces were determined directly by the height of the rupture peaks from curves of the adhesion force as function of distance using IgorPro 4.09 software (Wavemetrics, Lake Oswego, OR). Each loading rate (pN/second) applied to individual cadherin pairs was computed as the product of the slope of individual time-dependent force profiles prior to rupture (in pN/μm) and the reproach velocity (μm/second). Following Hanley et al. (Hanley et al., 2003), rupture force measurements were binned by increments of 50 pN/second for loading rates between 100 and 1000 pN/second and by increments of 500 pN/second for loading rates between 1000 and 10,000 pN/second. Each bin yields a mean rupture force. By plotting the mean rupture force as a function of loading rate, we could extract an unstressed dissociation rate and reactive compliance for different types of cadherin pairs (see Results section). These parameters characterize the binding interactions between cadherin molecules expressed on the surface of living cells at the single molecule level.

Cell aggregation assay

The extent of cell aggregation was obtained using the cell aggregation assay described (Meigs et al., 2002). Briefly, cells at 70-90% confluence were detached from the plate while preserving the cadherins (Brackenbury et al., 1981). Approximately 1×10^6 cells were placed in vials and rotated at 90 rpm, at 37°C. After 60 minutes, the formation of cell aggregates was analyzed by flow cytometry. Phase contrast microscopy (10× Plan Fluor objective; NA 0.3) was used to visualize

cell aggregates. We conducted two sets of control experiments: (1) cells were resuspended in PBS containing Ca^{2+}/Mg^{2+} with 5 mM EDTA; (2) In aggregation conditions, cells were resuspended in PBS containing Ca^{2+}/Mg^{2+}. Flow cytometry was used to determine the size distribution of cell aggregates and the potential effects of biotinylation on cell aggregation. CHO cells expressing N-cadherin were labeled with CMTMR (Molecular Probes, Eugene, OR). These labeled cells were then identified based on their forward-scatter, side-scatter and fluorescence profiles in a FACSCalibur flow cytometer, and aggregation was quantified as previously described (Hentzen et al., 2000; Jadhav et al., 2001; McCarty et al., 2002). The presence of aggregates did not clog the FACS apparatus, as the aperture of our FACSCalibur instrument is 100 μm, whereas a cell triplet is ~30-35 μm (e.g. Fig. 3C).

Fluorescence intensity of cadherin labeled with functional blocking antibody

To further investigate whether cadherin biotinylation affected our results, direct single-color immunofluorescence was used to compare the relative levels of expression of N-cadherin in control and biotinylated cells. N-cadherin monoclonal antibodies (Zymed, San Francisco, CA) were conjugated using a FITC protein labeling kit (Pierce). N-cadherin monoclonal antibodies were incubated with 1×10^6 cells suspension for 30 minutes at 25°C. The samples were then analyzed with a FACSCalibur flow cytometer. The geometric means of FITC fluorescence intensities were recorded.

Immunofluorescence microscopy

To visualize surface-expressed cadherins, cells were grown on glass-bottomed dishes and induced overnight with dexamethasone at a final concentration of 1 μM. All steps were performed at room temperature. Cells were blocked with 1% BSA in PBS for 20 minutes. Cells were then incubated for 30 minutes with either 1.5 μg/ml rat anti-E-cadherin or rat anti-N-cadherin monoclonal antibodies (Zymed) in 1% BSA in PBS. The cells were subsequently washed three times with 1% BSA in PBS and incubated for 5 minutes. The cells were then labeled with 0.027 μM DSB-X™ biotin goat anti-rat IgG (Molecular Probes) in 1% BSA in PBS for 30 minutes. After washing, the cells were incubated with tetramethylRhodamine-conjugated Neutravidin kindly provided by P. C. Searson (Johns Hopkins) at a final concentration of 0.025 mg/ml in 1% BSA in PBS. The cells were visualized with a 60×, oil-immersion objective mounted on an inverted epifluorescence microscope (Nikon, Melville, NY) (Kole et al., 2004).

Statistical analysis

Data are expressed as the mean ± s.e.m., unless otherwise stated. Statistical significance between the differences in the slopes of the force-displacement spectra was verified by pair-wise comparison using the Student's *t*-test. Values of $P<0.01$ were considered to be statistically significant. Mean values of the Bell's model parameters and corresponding standard deviations were tabulated by least-squares fits of the force versus log of loading rate coupled with the method of random-variable realizations.

We thank W. J. Nelson and G. G. Borisy for providing us with cell lines. This work was supported by a National Aeronautics and Space Administration grant NAG-1563 and National Institute of Health grants GM075305 and CA101135.

References

Adams, C. L. and Nelson, W. J. (1998). Cytomechanics of cadherin-mediated cell-cell adhesion. *Curr. Opin. Cell Biol.* **10**, 572-577.

Alon, R., Hammer, D. A. and Springer, T. A. (1995). Lifetime of P-selectin-carbohydrate bond in response to tensile force in hydrodynamic flow. *Nature* **374**, 539-542.

Altin, J. G. and Pagler, E. B. (1995). A one-step procedure for biotinylation and chemical cross-linking of lymphocyte surface and intracellular membrane-associated molecules. *Anal. Biochem.* **224**, 382-389.

Angres, B., Barth, A. and Nelson, W. J. (1996). Mechanism for transition from initial to stable cell-cell adhesion: kinetic analysis of E-cadherin-mediated adhesion using a quantitative adhesion assay. *J. Cell Biol.* **134**, 549-557.

Baumgartner, W., Hinterdorfer, P., Ness, W., Raab, A., Vestweber, D., Schindler, H. and Drenckhahn, D. (2000). Cadherin interaction probed by atomic force microscopy. *Proc. Natl. Acad. Sci. USA* **97**, 4005-4010.

Baumgartner, W., Schutz, G. J., Wiegand, J., Golenhofen, N. and Drenckhahn, D. (2003). Cadherin function probed by laser tweezer and single molecule fluorescence in vascular endothelial cells. *J. Cell Sci.* **116**, 1001-1011.

Bell, G. I. (1978). Models for the specific adhesion of cells to cells. *Science* **200**, 618-627.

Benoit, M., Gabriel, D., Gerisch, G. and Gaub, H. E. (2000). Discrete interactions in cell adhesion measured by single-molecule force spectroscopy. *Nat. Cell. Biol.* **2**, 313-317.

Brackenbury, R., Rutishauser, U. and Edelman, G. M. (1981). Distinct calcium-independent and calcium-dependent adhesion systems of chicken embryo cells. *Proc. Natl. Acad. Sci. USA* **78**, 387-391.

Cavellero, U. and Christofori, G. (2004). Cell adhesion and signalling by cadherins and Ig-CAMS in cancer. *Nat. Rev. Cell Mol. Biol.* **4**, 118-132.

Chang, M. I., Panorchan, P., Dobrowsky, T. M., Tseng, Y. and Wirtz, D. (2005). Single-molecule analysis of HIV-1 gp120-receptor interactions in living cells. *J. Virol.* **79**, 14748-14755.

Chappuis-Flament, S., Wong, E., Hicks, L. D., Kay, C. M. and Gumbiner, B. M. (2001). Multiple cadherin extracellular repeats mediate homophilic binding and adhesion. *J. Cell Biol.* **154**, 231-243.

Chausovsky, A., Bershadsky, A. D. and Borisy, G. G. (2000). Cadherin-mediated regulation of microtubule dynamics. *Nat. Cell Biol.* **2**, 797-804.

Chesla, S. E., Selvaraj, P. and Zhu, C. (1998). Measuring two-dimensional receptor-ligand binding kinetics by micropipette. *Biophys. J.* **75**, 1553-1572.

Chu, Y. S., Thomas, W. A., Eder, O., Pincet, F., Perez, E., Thiery, J. P. and Dufour, S. (2004). Force measurements in E-cadherin-mediated cell doublets reveal rapid adhesion strengthened by actin cytoskeleton remodeling through Rac and Cdc42. *J. Cell Biol.* **167**, 1183-1194.

Duguay, D., Foty, R. A. and Steinberg, M. S. (2003). Cadherin-mediated cell adhesion and tissue segregation: qualitative and quantitative determinants. *Dev. Biol.* **253**, 309-323.

Evans, E. (2001). Probing the relation between force–lifetime–and chemistry in single molecular bonds. *Annu. Rev. Biophys. Biomol. Struct.* **30**, 105-128.

Evans, E. and Ritchie, K. (1997). Dynamic strength of molecular adhesion bonds. *Biophys. J.* **72**, 1541-1555.

Gumbiner, B. M. (1996). Cell adhesion: the molecular basis of tissue architecture and morphogenesis. *Cell* **84**, 345-357.

Hanley, W., McCarty, O., Jadhav, S., Tseng, Y., Wirtz, D. and Konstantopoulos, K. (2003). Single molecule characterization of P-selectin/ligand binding. *J. Biol. Chem.* **278**, 10556-10561.

Hanley, W. D., Wirtz, D. and Konstantopoulos, K. (2004). Distinct kinetic and mechanical properties govern selectin-leukocyte interactions. *J. Cell Sci.* **117**, 2503-2511.

Hentzen, E. R., Neelamegham, S., Kansas, G. S., Benanti, J. A., McIntire, L. V., Smith, C. W. and Simon, S. I. (2000). Sequential binding of CD11a/CD18 and CD11b/CD18 defines neutrophil capture and stable adhesion to intercellular adhesion molecule-1. *Blood* **95**, 911-920.

Huber, O., Kemler, R. and Langosch, D. (1999). Mutations affecting transmembrane segment interactions impair adhesiveness of E-cadherin. *J. Cell Sci.* **112**, 4415-4423.

Hummer, G. and Szabo, A. (2001). Free energy reconstruction from nonequilibrium single-molecule pulling experiments. *Proc. Natl. Acad. Sci. USA* **98**, 3658-3661.

Hutter, J. L. and Beccoeffer, J. (1993). Calibration of atomic-force microscope tips. *Rev. Sci. Instr.* **64**, 1868-1873.

Ireton, R. C., Davis, M. A., van Hengel, J., Mariner, D. J., Barnes, K., Thoreson, M. A., Anastasiadis, P. Z., Matrisian, L., Bundy, L. M., Sealy, L. et al. (2002). A novel role for p120 catenin in E-cadherin function. *J. Cell Biol.* **159**, 465-476.

Jadhav, S., Bochner, B. S. and Konstantopoulos, K. (2001). Hydrodynamic shear regulates the kinetics and receptor specificity of polymorphonuclear leukocyte-colon carcinoma cell adhesive interactions. *J. Immunol.* **167**, 5986-5993.

Kole, T. P., Tseng, Y., Huang, L., Katz, J. L. and Wirtz, D. (2004). Rho kinase regulates the micromechanical response of adherent cells to Rho activation. *Mol. Biol. Cell* **15**, 3475-3484.

Konstantopoulos, K., Hanley, W. D. and Wirtz, D. (2003). Receptor-ligand binding: 'catch' bonds finally caught. *Curr. Biol.* **13**, R611-R613.

Makagiansar, I. T., Ikesue, A., Nguyen, P. D., Urbauer, J. L., Urbauer, R. J. and Siahaan, T. J. (2002). Localized production of human E-cadherin-derived first repeat in Escherichia coli. *Protein Expr. Purif.* **26**, 449-454.

Marshall, B. T., Long, M., Piper, J. W., Yago, T., McEver, R. P. and Zhu, C. (2003). Direct observation of catch bonds involving cell-adhesion molecules. *Nature* **423**, 190-193.

McCarty, O. J., Jadhav, S., Burdick, M. M., Bell, W. R. and Konstantopoulos, K. (2002). Fluid shear regulates the kinetics and molecular mechanisms of activation-dependent platelet binding to colon carcinoma cells. *Biophys. J.* **83**, 836-848.

Meigs, T. E., Fedor-Chaiken, M., Kaplan, D. D., Brackenbury, R. and Casey, P. J. (2002). Galpha12 and Galpha13 negatively regulate the adhesive functions of cadherin. *J. Biol. Chem.* **277**, 24594-24600.

Nelson, W. J. and Nusse, R. (2004). Convergence of Wnt, beta-catenin, and cadherin pathways. *Science* **303**, 1483-1487.

Niessen, C. M. and Gumbiner, B. M. (2002). Cadherin-mediated cell sorting not determined by binding or adhesion specificity. *J. Cell Biol.* **156**, 389-399.

Nose, A., Tsuji, K. and Takeichi, M. (1990). Localization of specificity determining sites in cadherin cell adhesion molecules. *Cell* **61**, 147-155.

Ozawa, M. (2002). Lateral dimerization of the E-cadherin extracellular domain is necessary but not sufficient for adhesive activity. *J. Biol. Chem.* **277**, 19600-19608.

Patel, S. D., Chen, C. P., Bahna, F., Honig, B. and Shapiro, L. (2003). Cadherin-mediated cell-cell adhesion: sticking together as a family. *Curr. Opin. Struct. Biol.* **13**, 690-698.

Perret, E., Leung, A., Feracci, H. and Evans, E. (2004). Trans-bonded pairs of E-cadherin exhibit a remarkable hierarchy of mechanical strengths. *Proc. Natl. Acad. Sci. USA* **101**, 16472-16477.

Pertz, O., Bozic, D., Koch, A. W., Fauser, C., Brancaccio, A. and Engel, J. (1999). A new crystal structure, Ca2+ dependence and mutational analysis reveal molecular details of E-cadherin homoassociation. *EMBO J.* **18**, 1738-1747.

Rahman, A., Tseng, Y. and Wirtz, D. (2002). Micromechanical coupling between cell surface receptors and RGD peptides. *Biochem. Biophys. Res. Commun.* **296**, 771-778.
Sako, Y., Nagafuchi, A., Tsukita, S., Takeichi, M. and Kusumi, A. (1998). Cytoplasmic regulation of the movement of E-cadherin on the free cell surface as studied by optical tweezers and single particle tracking: corralling and tethering by the membrane skeleton. *J. Cell Biol.* **140**, 1227-1240.
Shan, W. S., Tanaka, H., Phillips, G. R., Arndt, K., Yoshida, M., Colman, D. R. and Shapiro, L. (2000). Functional cis-heterodimers of N- and R-cadherins. *J. Cell Biol.* **148**, 579-590.
Shapiro, L. (2001). beta-catenin and its multiple partners: promiscuity explained. *Nat. Struct. Biol.* **8**, 484-487.
Shapiro, L., Fannon, A. M., Kwong, P. D., Thompson, A., Lehmann, M. S., Grubel, G., Legrand, J. F., Als-Nielsen, J., Colman, D. R. and Hendrickson, W. A. (1995). Structural basis of cell-cell adhesion by cadherins. *Nature* **374**, 327-337.
Shimoyama, Y., Takeda, H., Yoshihara, S., Kitajima, M. and Hirohashi, S. (1999). Biochemical characterization and functional analysis of two type II classic cadherins, cadherin-6 and -14, and comparison with E-cadherin. *J. Biol. Chem.* **274**, 11987-11994.
Shiraishi, K., Tsuzaka, K., Yoshimoto, K., Kumazawa, C., Nozaki, K., Abe, T., Tsubota, K. and Takeuchi, T. (2005). Critical role of the fifth domain of E-cadherin for heterophilic adhesion with {alpha}E{beta}7, but not for homophilic adhesion. *J. Immunol.* **175**, 1014-1021.
Sivasankar, S., Brieher, W., Lavrik, N., Gumbiner, B. and Leckband, D. (1999). Direct molecular force measurements of multiple adhesive interactions between cadherin ectodomains. *Proc. Natl. Acad. Sci. USA* **96**, 11820-11824.
Sivasankar, S., Gumbiner, B. and Leckband, D. (2001). Direct measurements of multiple adhesive alignments and unbinding trajectories between cadherin extracellular domains. *Biophys. J.* **80**, 1758-1768.
Takeichi, M. (1991). Cadherin cell adhesion receptors as a morphogenetic regulator. *Science* **251**, 1451-1455.
Tamura, K., Shan, W. S., Hendrickson, W. A., Colman, D. R. and Shapiro, L. (1998). Structure-function analysis of cell adhesion by neural (N-) cadherin. *Neuron* **20**, 1153-1163.
Wheelock, M. J., Soler, A. P. and Knudsen, K. A. (2001). Cadherin junctions in mammary tumors. *J. Mammary Gland Biol. Neoplasia* **6**, 275-285.
Yago, T., Wu, J., Wey, C. D., Klopocki, A. G., Zhu, C. and McEver, R. P. (2004). Catch bonds govern adhesion through L-selectin at threshold shear. *J. Cell Biol.* **166**, 913-923.
Yap, A. S. (1998). The morphogenetic role of cadherin cell adhesion molecules in human cancer: a thematic review. *Cancer Invest.* **16**, 252-261.
Yap, A. S., Brieher, W. M., Pruschy, M. and Gumbiner, B. M. (1997). Lateral clustering of the adhesive ectodomain: a fundamental determinant of cadherin function. *Curr. Biol.* **7**, 308-315.